


Article

Optimum, Suboptimal and Solar Sailing Orbital Maneuvers for a Spacecraft Orbiting the Earth

Lucas Gouvêa Meireles ^{1,†} , Vivian Martins Gomes ^{2,†}, Antônio Fernando Bertachini de Almeida Prado ^{1,3,*} and Cristiano Fiorilo de Melo ^{4,†}

¹ Postgraduate Division, National Institute for Space Research (INPE), Av. dos Astronautas, 1758, São José dos Campos 12227-900, SP, Brazil; meireleslg@gmail.com

² Department of Mathematics, São Paulo State University (UNESP), Av. Ariberto Pereira da Cunha, 333, Guaratinguetá 12516-410, SP, Brazil; vivian.gomes@unesp.br

³ Academy of Engineering, RUDN University, Miklukho-Maklaya Street 6, 117198 Moscow, Russia

⁴ Department of Mechanical Engineering, Federal University of Minas Gerais, Av. Antônio Carlos, 6627, Belo Horizonte 31270-901, MG, Brazil; cristiano.fiorilo@demec.ufmg.br

* Correspondence: antonio.prado@inpe.br

† These authors contributed equally to this work.

Abstract: The present research performs numerical studies to search for the best maneuvers, from the point of view of minimum time, to make adjustments in the semi-major axis, eccentricity and inclination of a spacecraft traveling around the Earth. For those maneuvers, low thrust propulsion is used under optimal and sub-optimal assumptions, to verify the main differences in terms of transfer time. In addition, solar sail dynamics is used. The spacecraft is assumed to have a propulsion with a fixed magnitude and that the control is based on choosing the direction of the propulsion. It is found that optimal control gives the minimum transfer time, while sub-optimal control restricted the control to follow a prescribed function, which is assumed to be a constant or linear function in time. Finally, solar sails present themselves as an option where fuel is a critical factor, given their much longer maneuver duration, but with a zero fuel consumption. The numerical-analytical modeling of optimization methods developed in this study can break any type of symmetry in the solutions. In turn, they can increase their energetic efficiency. The present research compares those results in detail, in particular looking at the transfer time in all cases studied.

Keywords: astrodynamics; maximum principle of Pontryagin; optimal control; orbital mechanics; solar sailing



Citation: Meireles, L.G.; Gomes, V.M.; Prado, A.F.B.d.A.; Melo, C.F.d. Optimum, Suboptimal and Solar Sailing Orbital Maneuvers for a Spacecraft Orbiting the Earth. *Symmetry* **2023**, *15*, 512. <https://doi.org/10.3390/sym15020512>

Academic Editor: Chong Wang

Received: 23 January 2023

Revised: 3 February 2023

Accepted: 8 February 2023

Published: 14 February 2023



Copyright: © 2023 by the authors. Licensee MDPI, Basel, Switzerland. This article is an open access article distributed under the terms and conditions of the Creative Commons Attribution (CC BY) license (<https://creativecommons.org/licenses/by/4.0/>).

1. Introduction

An orbital maneuver occurs when a spacecraft is moved from one orbit to another through the use of propulsion systems. There are many reasons to perform this task, such as changing the application of a spacecraft or just making corrections to keep it in the desired orbit, with applications such as Canuto et al. [1]. It is also common that the launcher delivers the spacecraft in an orbit that is not the final one due to limitations of the launch vehicles. In this case, an orbital maneuver is required. It is also common to specify transfers with minimum time or fuel expenditure because both of them are very important in space missions.

Recent advances in space technologies have made it possible to perform these maneuvers with no fuel expenditure, by using solar sail spacecrafts [2–7]. These vehicles absorb the linear momentum of sunlight and use it as its own form of propulsion [8].

Thus, our general problem is an optimization problem that consists of changing the initial state of a spacecraft (position and velocity) from $\mathbf{r}_0, \mathbf{v}_0$ at the time t_0 , to the final state $\mathbf{r}_f, \mathbf{v}_f$ at the time t_f ($t_f > t_0$) using the minimum possible time for the transfer. When using propulsion, there is a cost in terms of fuel to make these maneuvers. Additionally, a zero

fuel expenditure study is implemented with the use of a solar sail, in order to compare the transfer time and orbits achieved.

In principle, in a low thrust maneuver, it is possible to choose the direction and magnitude of the thrust to be applied in the spacecraft at every instant of time, but this is a solution that is usually very hard to implement. In order to do that, it is necessary to control the attitude of the satellite and very fast variations of attitude are required, if the thruster is fixed to the satellite structure. Even if it is not fixed, it is still complicated to implement a general law for the direction of the thrust.

Therefore, the present paper compares the optimal control version with the sub-optimal one, where the magnitude of the thrust is constant and the direction is constant or follows a linear relation with an angle that describes the position of the spacecraft. This second case represents a situation that is easier to implement. After that, the same maneuver is simulated using a solar sail, and the results are compared.

In a sense, this paper is a continuation of Prado [9], by comparing optimal control with a suboptimal solution that uses only one arc for the propulsion, using fuel consumption as the criterion to be minimized. The main new aspect of the present paper is the use of a solar sail to perform the same maneuver. Given the propellant-less propulsion offered by solar sails, it is possible to reduce even further the fuel consumption established by the optimal solution. The challenge is verifying if the solar sail can make this maneuver, given its thrust direction restrictions, and how much time it requires.

In summary, this paper presents studies of numerical-analytical modeling, such as [10–12], and their application on efficient optimization methods in mechanics and control problems of space missions. Those methods can break any type of symmetry in the trajectories obtained, but increase their energetic efficiency.

2. Model Used

For the maneuvers based on low thrust constant propulsion, the spacecraft is considered to be traveling with its equations of motion obtained from the forces that are present in the system, which are: the gravity field of the Earth, assumed to be Keplerian, and the thrust, when turned on. The thrust is established with a fixed magnitude, totally free direction (for the optimal control version of the maneuver) and constant or with linear variation of the angular motion (for the suboptimal control versions of the maneuver). The thrust is assumed to be working all the time in all versions of the problem. Afterwards, the solutions pursued are the direction that the thrust should be applied as a function of time and the respective transfer time of the maneuver.

The formulation of the problem can be written as:

- Objective Function: T ,
where T is the time of transfer, the variable to be minimized with respect to the control;
- Subject to: Equations of motion, constraints in the state and control.

For the suboptimal version, the direction of the application of the thrust (the control) can be represented by a linear function of the true anomaly of the spacecraft, which is an angle that defines the position of the spacecraft [13,14]. The direction of the thrust (the planar angle of pitch (A) and the out-of-plane angle of yaw (B), both angles considering the orbital plane of the spacecraft as the fundamental plane of reference) can be expressed by Equations (1) and (2). The “pitch” (A) is the angle of the projection of the thrust vector in the orbital plane. It is measured from the circumferential direction in a clockwise rotation, such that a thrust with $A = 90^\circ$ is given in the radial direction pointing away from the central body. The “yaw” (B) is the angle between the thrust vector and its projection in the orbital plane:

$$A = A_0 + A' * (s - s_s) \quad (1)$$

$$B = B_0 + B' * (s - s_s) \quad (2)$$

where A_0, B_0, A', B' are constants to be found, s is the range angle of the spacecraft, and s_s represents the range angle of the spacecraft when the thrust is turned-on. The range angle is just an angle that gives the position of the spacecraft with respect to a given point to start the measurements. When $A' = B' = 0$, we have a constant direction of thrust.

In this format, we have four or six variables to be optimized (the true anomalies of starting and ending of the thruster and A_0, B_0, A', B'). The case that only four variables need to be optimized is when thrust is given in a constant direction, such that $A' = B' = 0$.

We can use here the same set of variables used in Prado [9], which are shown hereinafter:

$$\begin{cases} X_1 = [a(1 - e^2)/\mu]^{1/2} \\ X_2 = e \cos(\omega - \phi) \\ X_3 = e \sin(\omega - \phi) \\ X_4 = (\text{Fuel consumed})/m_0 \\ X_5 = t \\ X_6 = \cos(i/2) \cos((\Omega + \phi)/2) \\ X_7 = \sin(i/2) \cos((\Omega - \phi)/2) \\ X_8 = \sin(i/2) \sin((\Omega - \phi)/2) \\ X_9 = \cos(i/2) \sin((\Omega + \phi)/2) \\ \phi \equiv \nu + \omega - s \end{cases} \tag{3}$$

where s is the range angle of the spacecraft, which is the angle between the position vector of the spacecraft and a generic reference line in the orbital plane, a is the semi-major axis, e is the eccentricity, i is the inclination, ω is the argument of periapsis, ν is the true anomaly of the spacecraft, Ω is the argument of the ascending node, and ϕ is defined by its equation. The reason why the spacecraft position is both represented by the true anomaly and the range angle is to maintain the same notation as Biggs [14,15].

In those variables, the equations of motion are:

$$\begin{cases} dX_1/ds = f_1 = SiX_1F_1 \\ dX_2/ds = f_2 = Si\{[(Ga + 1) \cos(s) + X_2]F_1 + GaF_2 \sin(s)\} \\ dX_3/ds = f_3 = Si\{[(Ga + 1) \sin(s) + X_3]F_1 - GaF_2 \cos(s)\} \\ dX_4/ds = f_4 = SiGaF(1 - X_4)/(X_1W) \\ dX_5/ds = f_5 = SiGa(1 - X_4)m_0/X_1 \\ dX_6/ds = f_6 = -SiF_3[X_7 \cos(s) + X_8 \sin(s)]/2 \\ dX_7/ds = f_7 = SiF_3[X_6 \cos(s) - X_9 \sin(s)]/2 \\ dX_8/ds = f_8 = SiF_3[X_9 \cos(s) + X_6 \sin(s)]/2 \\ dX_9/ds = f_9 = SiF_3[X_7 \sin(s) - X_8 \cos(s)]/2 \end{cases} \tag{4}$$

where

$$\begin{cases} Ga = 1 + X_2 \cos(s) + X_3 \sin(s) \\ Si = (\mu X_1^4)/[Ga^3 m_0(1 - X_4)] \\ F_1 = F \cos(A) \cos(B) \\ F_2 = F \sin(A) \cos(B) \\ F_3 = F \sin(B) \end{cases} \tag{5}$$

where F is the magnitude of the force, and W is the ejection speed of the gases.

We also have the constraints given by the fact that the spacecraft has to reach a final orbit and leave from a given initial orbit.

3. Optimal Solution

The optimal solution can be obtained using optimal control theory [16]. We can write first order necessary conditions to have a local minimum and, from there, we can obtain:

- (a) The differential equations that give the Lagrange multipliers, called “adjoint equations”. When we combine them with the equations of motion, we have a complete set of differential equations that solves the problem;
- (b) The “Transversality Conditions”, which are the conditions that the Lagrange multipliers must achieve at the end of the numerical integration. They complete the conditions to be satisfied by the solution of the problem when combined to the fact that the maneuver starts at a given initial orbit and ends in a different final orbit;
- (c) The “Maximum Principle of Pontryagin”, which states that it is necessary to maximize the magnitude of the scalar product of the Lagrange multipliers with the right-hand side of the equations of motion. This point gives the condition to find the optimal angles of “pitch” and “yaw” at each instant of time.

This problem can be solved using the algorithm described in the next steps:

- (i) Give estimates for the initial and final times of the maneuver and the initial values of the Lagrange multipliers;
- (ii) Make a numerical integration of the adjoint equations and the equations of motion, using the values for the “pitch” and “yaw” angles obtained from the Maximum Principle of Pontryagin;
- (iii) After that, check if the boundary conditions are satisfied. If not, update the initial values and start again. This update is explained in further detail in Section 4 with the use of Equations (9) and (10). If the conditions are satisfied, the solution was found.

The adjoint equations are:

$$\left\{ \begin{aligned} \frac{dp_1}{ds} &= -\frac{1}{X_1} \left[4 \sum_{j=1}^9 p_j f_j + p_1 f_1 - p_4 f_4 - p_5 f_5 \right] \\ \frac{dp_2}{ds} &= \frac{\cos(s)}{Ga} \left[3 \sum_{j=1}^9 p_j f_j - p_4 f_4 - p_5 f_5 \right] - Si p_2 F_1 \\ &\quad - Si \cos^2(s) (p_2 F_1 - p_3 F_2) - Si \cos(s) \sin(s) (p_2 F_2 + p_3 F_1) \\ \frac{dp_3}{ds} &= \frac{\sin(s)}{Ga} \left[3 \sum_{j=1}^9 p_j f_j - p_4 f_4 - p_5 f_5 \right] - Si p_3 F_1 \\ &\quad - Si \cos(s) \sin(s) (p_2 F_1 - p_3 F_2) - Si \sin^2(s) (p_2 F_2 + p_3 F_3) \\ \frac{dp_4}{ds} &= -\frac{1}{m_0(1 - X_4)} \left[\sum_{j=1}^9 p_j f_j - p_4 f_4 - p_5 f_5 \right] \\ \frac{dp_5}{ds} &= 0 \\ \frac{dp_6}{ds} &= -\frac{Si F_3}{2} [p_7 \cos(s) + p_8 \sin(s)] \\ \frac{dp_7}{ds} &= \frac{Si F_3}{2} [p_6 \cos(s) - p_9 \sin(s)] \\ \frac{dp_8}{ds} &= \frac{Si F_3}{2} [p_6 \sin(s) + p_9 \cos(s)] \\ \frac{dp_9}{ds} &= -\frac{Si F_3}{2} [p_8 \cos(s) - p_7 \sin(s)] \end{aligned} \right. \tag{6}$$

where p_i are the Lagrange multipliers.

The condition that comes from the Principle of Pontryagin can be written as:

- Extremize $\sum_{i=1}^9 p_i f_i$ with respect to A .

To obtain the values of A at every instant of time, it is necessary to make the derivatives of f_i with respect to A and set them to zero [15]. Doing so, we have:

$$\sin(A) = q_2/S' \tag{7a}$$

$$\cos(A) = q_1/S' \tag{7b}$$

where:

$$\begin{cases} S' = \pm\sqrt{q_1^2 + q_2^2} \\ q_1 = p_1X_1 + p_2[X_2 + (Ga + 1) \cos(s)] + p_3[X_3 + (Ga + 1) \sin(s)] \\ q_2 = p_2Ga \sin(s) - p_3Ga \cos(s) \end{cases} \tag{8}$$

4. Numerical Method

The solution of the nonlinear programming problem can be found using the gradient projection method [17,18]. This method is based on selecting an initial guess for all the components of the vector \mathbf{X} , which we call \mathbf{X}_0 . Using this vector, we make a numerical integration of the trajectory to find the vector \mathbf{X} at the final time. At this point, two steps are taken:

- (i) First, we need to make the system satisfy the constraints given by the problem (usually some orbital elements of the final orbit). For this step, we use the update:

$$\mathbf{X}_{i+1} = \mathbf{X}_i - \nabla \mathbf{f}^T \cdot [\nabla \mathbf{f} \cdot \nabla \mathbf{f}^T]^{-1} \mathbf{f} \tag{9}$$

where \mathbf{f} is the vector formed by the active constraints;

- (ii) After the constraints are satisfied, we take some steps to minimize the fuel consumed. For this phase, the updates are given by:

$$\mathbf{X}_{i+1} = \mathbf{X}_i + \left(\gamma \frac{J(\mathbf{X})}{\nabla J(\mathbf{X}) \cdot \mathbf{d}} \right) \frac{\mathbf{d}}{|\mathbf{d}|} \tag{10}$$

with:

$$\mathbf{d} = -\left(\mathbf{I} - \nabla \mathbf{f}^T [\nabla \mathbf{f} \cdot \nabla \mathbf{f}^T]^{-1} \mathbf{f} \right) \cdot \nabla J(\mathbf{X}) \tag{11}$$

where \mathbf{I} is the unit matrix, \mathbf{d} is the search direction, J is the fuel consumed, and γ is a parameter that controls the convergence speed of the optimization problem. Large values increase the convergence speed, but reduce the accuracy of the solution because there are larger oscillations around the real solution of the problem. On the other side, lower values require more steps until a convergence is obtained, but the solution is more accurate.

In both iterations, this procedure continues until $|\mathbf{X}_{i+1} - \mathbf{X}_i| < \varepsilon$, where ε is a given tolerance that represents the accuracy required for the solution.

5. Solar Sailing

The solar sail spacecraft dynamics is initially defined in a Spacecraft Oriented Frame (SOF), with an origin at the barycenter of the spacecraft. Its X-axis corresponds to the direction of the incoming sunlight (\mathbf{u}). The Z-axis points in the direction of the cross product of the position and the velocity of the spacecraft, both in respect to the Sun. Finally, the Y-axis is defined in agreement with a coordinate system in dextrorotation.

The angles that determine the orientation of the solar sail, defined by the vector normal to its surface (\mathbf{n}), are called azimuth (α) and elevation (δ). The azimuth (α) is the angle between the projection of \mathbf{n} on the XY-plane ($proj_{XY}\mathbf{n}$) and \mathbf{u} . The elevation (δ) is the angle between \mathbf{n} and $proj_{XY}\mathbf{n}$.

The resulting Solar Radiation Pressure (SRP) thrust (**T**) is defined as a function of **n**. In order to determine its value, it is convenient to make use of the lightness vector **L** (Equation (12)), defined as the SRP acceleration normalized by the local gravitational acceleration of the Sun [19]:

$$\mathbf{L} = \left(\frac{1}{2} \frac{\sigma_c}{\sigma}\right) n_x [(2r_{\text{spec}}n_x + \chi_f r_{\text{diff}} + \kappa a_{\text{bsor}})\mathbf{n} + (a_{\text{bsor}} + r_{\text{diff}})\mathbf{u}] \tag{12}$$

where σ_c is a constant referred to as critical loading (Equation (13)), σ is the sail loading (Equation (14)), n_x is the **n** X-axis component, a_{bsor} , r_{spec} and r_{diff} are, respectively, the absorptance, specular reflectance and diffuse reflectance coefficients, χ is another coefficient related to emission/diffusion, and κ is a dimensionless factor, which results from the net thrust of the absorbed and re-emitted radiation on the two sides of the sail. The subscripts “f” and “b” refer to the front and back side of the sail.

$$\sigma_c \equiv 2 \frac{I_{1\text{AU}}}{c g_{1\text{AU}}} \approx 1.5368 \text{ g/m}^2 \tag{13}$$

$$\sigma \equiv \frac{m}{A} \tag{14}$$

$$\kappa \equiv \frac{\chi_f \epsilon_f(T) - \chi_b \epsilon_b(T)}{\epsilon_f(T) + \epsilon_b(T)} \tag{15}$$

where $I_{1\text{AU}} = 1366 \text{ W/m}^2$ and $g_{1\text{AU}} \approx 5.930 \times 10^{-3} \text{ m/s}^2$ are both constants which represent, respectively, the energy flux emitted by the Sun and its gravitational acceleration, both at 1 au, $c \approx 2.9979 \times 10^8 \text{ m/s}$ is the speed of light in vacuum, m is the total mass of the spacecraft, A and T are, respectively, the solar sail surface area and its temperature and ϵ is the solar sail emittance coefficient.

The values for the optical coefficients were taken from solar sail models made in the early 2000s by the Jet Propulsion Laboratory [20]. The values considered were $a_b = 0.12$, $r_{\text{spec}} = 0.8272$, $r_{\text{diff}} = 0.0528$, $\epsilon_f = 0.05$, $\epsilon_b = 0.55$, $\chi_f = 0.79$ and $\chi_b = 0.55$.

Finally, this study considered a sail loading of $\sigma = 198.7 \text{ g/m}^2$. This value is calculated from Equation (16) and was taken from the effective lightness number ($\beta = 0.0077$) of the ACS3 mission from NASA [21]:

$$\beta = \frac{\sigma_c}{\sigma} \tag{16}$$

Sail Attitude Strategy

The sail orientation strategy used for the azimuth α is taken from McInnes [20] and further implemented in Meireles et al. [22]. Even though the spacecraft orbits the Earth, it is necessary to know the spacecraft distance to the Sun to determine \mathbf{a}_{SRP} . Therefore, the dynamics take place in a Heliocentric Inertial Frame in a three-body gravitational problem (Sun, Earth and Solar Sail Spacecraft). The strategy consists of maintaining half a rotation per orbital revolution around the Earth. In order to avoid big attitude maneuvers, the sail is considered to have both of its sides made of reflective materials. This strategy can be broken down into two modes of operation:

- (i) Increase the spacecraft orbital energy, where the resulting SRP force is directed to the direction of the spacecraft geocentric velocity (as illustrated in Figure 1);
- (ii) Decrease the spacecraft orbital energy, where the resulting SRP force is directed in the opposite direction of the spacecraft geocentric velocity (as illustrated in Figure 2).

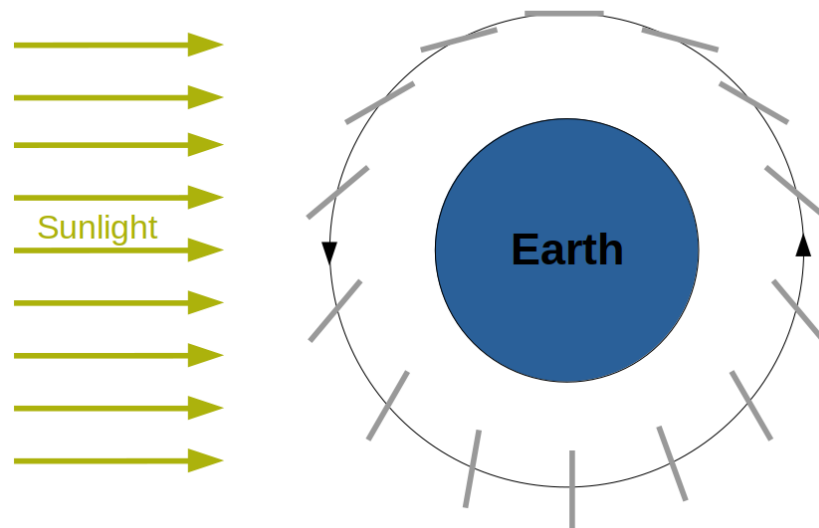


Figure 1. Strategy (i).

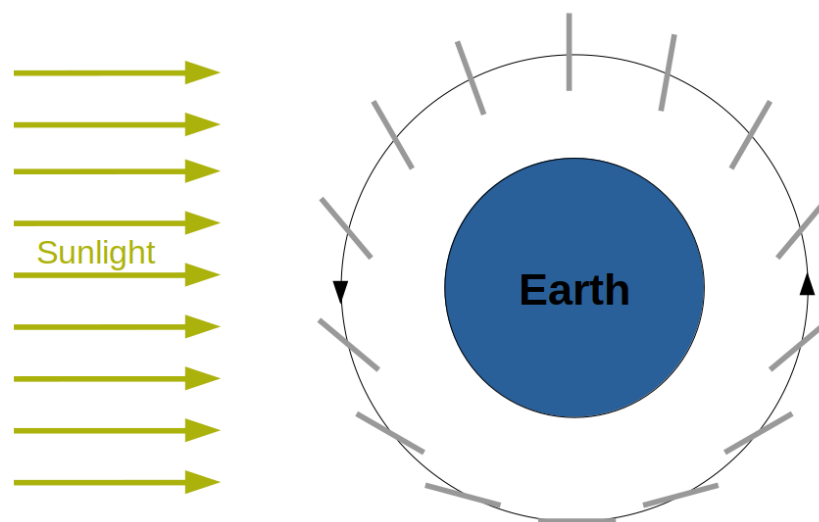


Figure 2. Strategy (ii).

At each instant t , the $\alpha(t)$ and $\delta(t)$ are determined as follows, in order to correct the required orbital elements of the spacecraft:

- Semi-major axis $\rightarrow a_{ref}$:
 - If $a(t) < a_{ref}$: implement Strategy (i);
 - If $a(t) > a_{ref}$: implement Strategy (ii);
- Eccentricity $\rightarrow e_{ref}$:
 - If $e(t) < e_{ref}$: implement Strategy (i) if the spacecraft geocentric eccentricity vector \mathbf{e} points in the opposite direction of the Earth velocity and Strategy (ii) if otherwise;
 - If $e(t) > e_{ref}$: implement Strategy (i) if \mathbf{e} points in the direction of the Earth velocity and Strategy (ii) if otherwise;
- Inclination $\rightarrow i_{ref}$:
 - If $i(t) < i_{ref}$: $\delta_{geo} = +35^\circ$ if the spacecraft geocentric true longitude is $\nu \approx 0^\circ$ and $\delta_{geo} = -35^\circ$ if $\nu \approx 180^\circ$;

- If $i(t) > i_{ref}$: $\delta_{geo} = -35^\circ$ if $\nu \approx 0^\circ$ and $\delta_{geo} = +35^\circ$ if $\nu \approx 180^\circ$,

where δ_{geo} is the elevation angle of the sail considering a fundamental plane of reference as the spacecraft geocentric orbital plane. The elevation angle δ in the SOF is defined as a consequence.

6. Results

To verify the applicability of the methods proposed here, we now make simulations of orbital maneuvers using all of them. The results obtained in Sections 6.1 and 6.2 are in accordance with Biggs [14,15]. The solar sail performance in Section 6.3 is in line with the latest solar sail mission data made available by The Planetary Society [23].

This test case was simulated from a deviated geostationary orbit, which suffered a small altitude decay and increase in eccentricity and inclination. Geostationary orbits are sensible to third body perturbations and frequently need orbital corrections. In this case, the corrections are made with a continuous and constant low thrust. The problem is defined in the Earth Centered Inertial frame (ECI) and taken from a previous case study from Biggs [15] with the following data:

- Initial orbit:
 - Semi-major axis: 41,904.1 km;
 - Eccentricity: 0.018;
 - Inclination: 0.688° ;
 - Ascending node: -29.8° ;
 - Argument of perigee: 7.0° .
- Initial data:
 - Total mass (vehicle + fuel): 300 kg;
 - Magnitude of thrust available: 2 N.
- Imposed conditions of final (geostationary) orbit:
 - Semi-major axis: 42,164.2 km;
 - Eccentricity: 0.0;
 - Inclination: 0.0° .

6.1. Optimal Maneuver

The first method to be tested is the “optimal” one, since it gives the actual minimum time for the transfer, and the results can be used to verify the other methods. The goal is to correct deviations from a circular and equatorial orbit and to increase the semi-major axis. To use the optimal maneuver, we have the data shown next:

- Constraint satisfaction tolerance: 0.03;
- Initial guess:
 - Propulsion start: 100.0° ;
 - Propulsion end: 110.0° ;
 - Initial pitch angle: 180.0° ;
 - Initial yaw angle: -45.0° ;
 - Initial pitch rate of change: 0.5;
 - Initial yaw rate of change: 0.0.

The initial guess values are a consequence of a trial and error process.

The obtained optimal values for “pitch” and “yaw” angles are displayed in Figure 3.

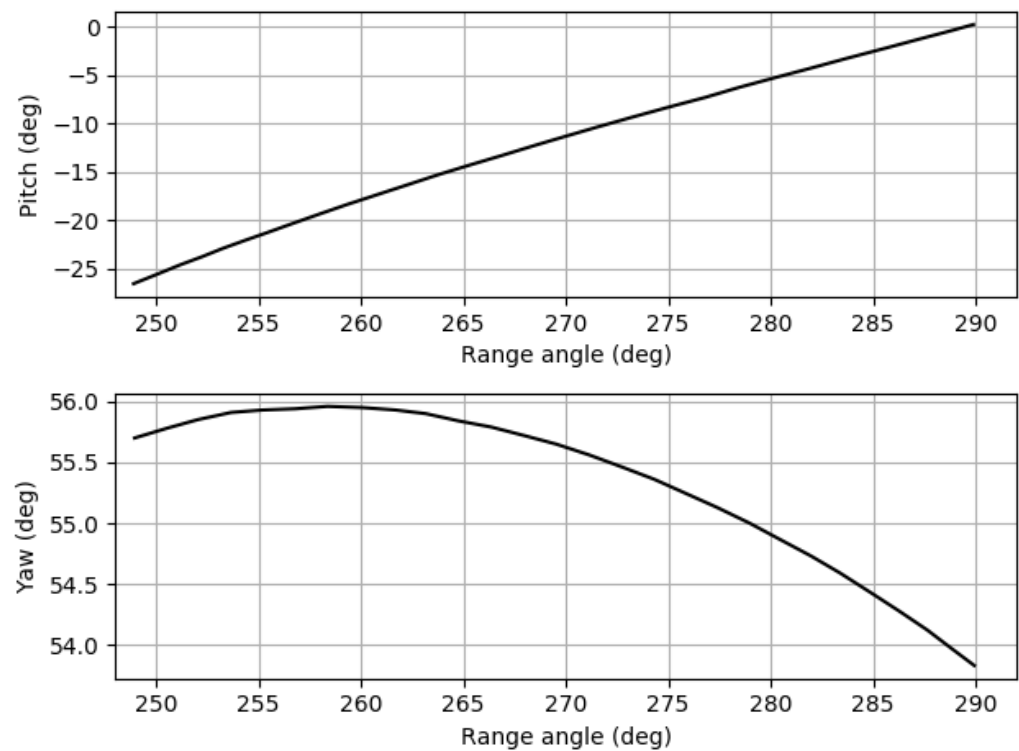


Figure 3. Optimal pitch and yaw angle values.

- Effectively achieved orbit:
 - Semi-major axis: 42,161.23 km;
 - Eccentricity: 0.000;
 - Inclination: 0.0°;
 - Ascending node: 265.5°;
 - Argument of perigee: 93.2°;
 - True anomaly: 171.8°.
- Duration of the maneuver: 15,237.6 s.

It is important to remember that the duration of the maneuver is taken from the integration of f_5 from Equation (4).

The results showed that the method converged very well with the initial guess proposed. Besides that, we also see that the “pitch” angle is almost linear, which indicates that sub-optimal solutions will work very well. The “yaw” angle is clearly not linear. However, it changes in a range of 54–56 degrees, so may be approximated with a constant value or constant with small linear variation. The most important result is the minimum time of the transfer, which is 15 237.6 s, about 253.96 min or 4.23 h. It is important to mention that this is not the burning time of the propulsion arc because this time is counted from the initial true anomaly of the spacecraft, and the optimization algorithm chooses the best point to start the propulsion, which is not the initial true anomaly of the spacecraft. The burning has a length of about 41 degrees, starting at $s_s = 249^\circ$ and ending at $s_e = 290^\circ$, as shown by Figure 3.

6.2. Suboptimal Maneuvers

The next step is to make the same maneuver using two versions of the suboptimal technique. The first one considers that the direction of the thrust can have a linear variation with the range angle (or the true anomaly of the spacecraft, since the difference between them is a constant), and the second one assumes a constant value for the direction.

The results are shown in Table 1. This table gives the start (s_s) and end (s_e) of the propulsion (in terms of the range angles), the values of the constants involved (A_0 , B_0 , A' , B' for the linear variations or A_0 , B_0 , for the constant direction and the optimal maneuver) and the transfer time in seconds.

Table 1. Suboptimal transfers.

Maneuver	s_s ($^\circ$)	s_e ($^\circ$)	A_0 ($^\circ$)	B_0 ($^\circ$)	A'	B'	Duration (s)
Optimal	249	290	−26.6	55.7	-	-	15,237.6
Linear	235	282	−22	45	0.687	0.067	17,121.3
Constant	221	271	−12	55	0	0	18,305.4

The linear approximation requires a larger burning arc, 47 degrees against 41 degrees for the optimal maneuver, and has a transfer time of 17,121.3 s (285.35 min or 4.76 h), an increase of 1883.7 s or 31.40 min. Those results show that the linear approximation is a very good choice because it does not increase the transfer time too much. In terms of fuel consumption, although it is not the goal of the present paper, the difference is proportional because the thrust has constant magnitude and is active all the time. It means an increase of 12.36%.

When considering the constant direction for the propulsion, this approximation requires a little bit larger burning arc, 50 degrees and has a transfer time of 18,305.4 s (305.09 min or 5.09 h). This means an increase of 3067.8 s or 51.13 min. Those results show that this approximation is also an interesting choice because it does not increase too much the transfer time. In terms of fuel consumption, it means an increase of 20.13%.

As a summary, both techniques based in a constant low thrust propulsion show good results, with faster transfer times. The differences among these techniques are between 12% and 20%, which can be acceptable for many missions considering the simplification of the control. The next step is to study how to make this maneuver using a solar sail, which does not use fuel.

6.3. Solar Sail Spacecraft

The progress of the values of the spacecraft geocentric orbital elements over time are displayed by the black full lines in Figure 4. The red dashed lines indicate their initial values and the blue dashed lines their given final values.

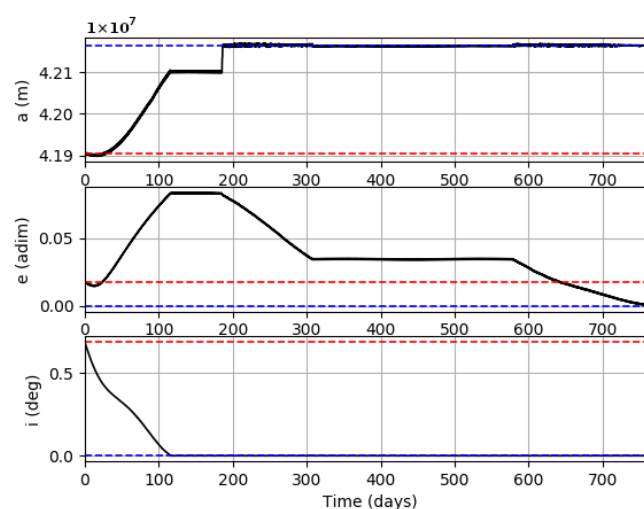


Figure 4. Orbital elements of the spacecraft over time. (Red line: initial value; Blue line: final value).

It can be seen that the solar sail was able to correct the inclination in approximately 116 days, the semi-major axis in 185 days, and the eccentricity in 770 days.

The eccentricity can only be corrected in certain moments because it depends on the relative positions between the Sun, the Earth and the Spacecraft. This justifies the long idle periods between the days 115 through 185 and 305 through 580. Additionally, the eccentricity must be the last orbital element to be corrected because it is affected by the correction of the others. The long time required to correct the eccentricity is a consequence of these reasons.

The azimuth α and elevation δ values of the sail over time are displayed in Figure 5.

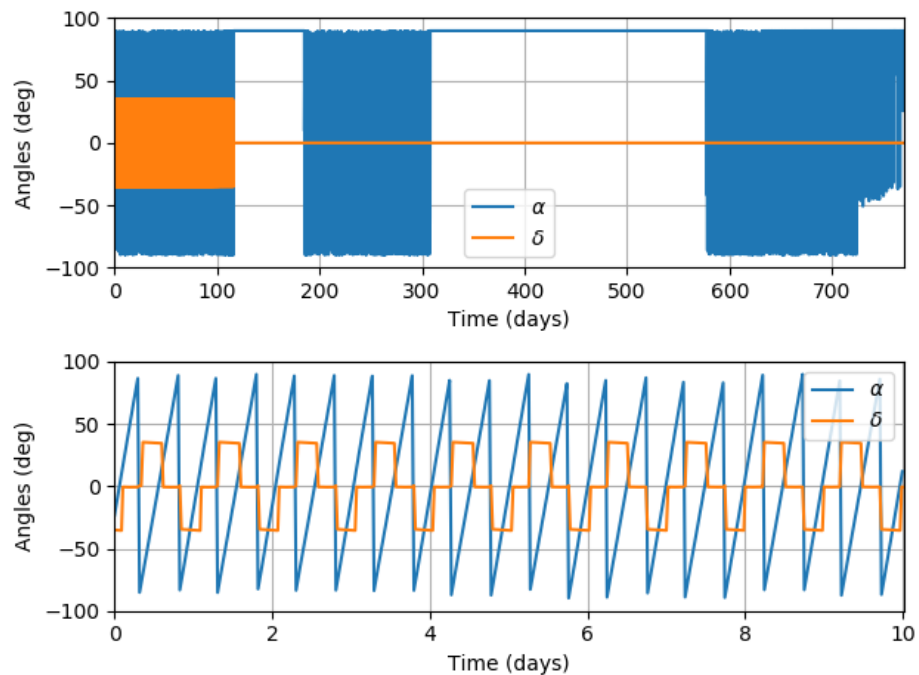


Figure 5. Solar sail attitude angles over time.

The long idle periods of the solar sail, with no exposed surface area to the sunlight ($\alpha = 90^\circ$) and, consequently, a null SRP force, can be verified by this plot. Due to the long transfer time, it can be difficult to observe the behavior of α and δ in greater detail. The variation of their values through the course of a day appears as a blur when represented throughout the entire time frame of the maneuver. Therefore, a second plot is displayed for a shorter period of 10 days (zoom in on the X-axis).

The duration of the maneuver is: 66,528,000 s (770 days), which is $4366\times$ greater than the optimal minimum time transfer. In compensation, the solar sail offers the possibility of zero fuel consumption and presents itself as a viable option when fuel consumption is a critical factor compared to the orbital maneuver duration.

7. Conclusions

The present paper worked with station-keeping maneuvers for a spacecraft around the Earth. The goal was to correct deviations in semi-major axis, eccentricity and inclination. Three techniques were implemented: linear and constant suboptimal control, optimal control maneuvers (both of them using a constant thrust magnitude) and propulsion based on solar sails. The criterion is to minimize transfer time, which is the equivalent of minimizing fuel consumption for the maneuvers based on propulsion. All of them proved to be successful in achieving a predetermined final orbit, even with a semi-major axis, eccentricity and inclination constraints.

The results show clearly that the optimal maneuver has the minimum time transfer, but suboptimal linear control has a 12.36% greater transfer time. However, it has a much simpler hardware implementation. Going for a constant direction of thrust, we have an extra 7.77% in transfer time but a much easier implementation of the control. Regarding fuel consumption, the differences are the same. Thus, those possibilities are available for a mission designer.

Solar sails present an advantage, which is the zero fuel consumption. However, they demand a much longer time ($4366\times$ greater) to perform the necessary maneuver. In the simulation analyzed, it was able to correct the inclination in a little over 116 days, the semi-major axis in around 185 days and the eccentricity in approximately 770 days. It is clear that the process is much faster if only semi-major axis and inclination need to be corrected.

The final decision on which method to use depends on the requirements of the mission, both in terms of transfer time and fuel available. It also depends on the magnitude of the corrections and the Keplerian elements to be corrected.

Author Contributions: Conceptualization, L.G.M., V.M.G. and A.F.B.d.A.P.; methodology, L.G.M., V.M.G. and A.F.B.d.A.P.; software, L.G.M., V.M.G. and A.F.B.d.A.P.; validation, A.F.B.d.A.P. and C.F.d.M.; formal analysis, A.F.B.d.A.P. and C.F.d.M.; investigation, L.G.M., V.M.G. and A.F.B.d.A.P.; resources, A.F.B.d.A.P.; data curation, L.G.M. and A.F.B.d.A.P.; writing—original draft preparation, L.G.M., V.M.G. and A.F.B.d.A.P.; writing—review and editing, A.F.B.d.A.P. and C.F.d.M.; visualization, L.G.M., V.M.G., A.F.B.d.A.P. and C.F.d.M.; supervision, A.F.B.d.A.P.; project administration, A.F.B.d.A.P.; funding acquisition, A.F.B.d.A.P. All authors have read and agreed to the published version of the manuscript.

Funding: This research was funded by the National Council for Scientific and Technological Development (CNPq) Grant No. 309089/2021-2, by the São Paulo Research Foundation (FAPESP) Grant Nos. 2016/24561-0 and 2018/19959-0 and by the RUDN University Scientific Projects Grant System, Project No. 202235-2-000.

Institutional Review Board Statement: Not applicable.

Informed Consent Statement: Not applicable.

Data Availability Statement: The data presented in this study are available on request from the corresponding author.

Acknowledgments: The authors wish to express their appreciation for the support provided by the National Council for the Improvement of Higher Education (CAPES).

Conflicts of Interest: The authors declare no conflict of interest. The funders had no role in the design of the study; in the collection, analyses, or interpretation of data; in the writing of the manuscript; or in the decision to publish the results.

References

1. Canuto, E.; Molano-Jimenez, A.; Perez-Montenegro, C.; Massotti, L. Long-distance, drag-free, low-thrust, LEO formation control for Earth gravity monitoring. *Acta Astronaut.* **2011**, *69*, 571–582. [[CrossRef](#)]
2. Funase, R.; Shirasawa, Y.; Mimasu, Y.; Mori, O.; Tsuda, Y.; Saiki, T.; Kawaguchi, J. On-orbit verification of fuel-free attitude control system for spinning solar sail utilizing solar radiation pressure. *Adv. Space Res.* **2011**, *48*, 1740–1746. [[CrossRef](#)]
3. Tsuda, Y.; Mori, O.; Funase, R.; Sawada, H.; Yamamoto, T.; Saiki, T.; Endo, T.; Yonekura, K.; Hoshino, H.; Kawaguchi, J. Achievement of IKAROS—Japanese deep space solar sail demonstration mission. *Acta Astronaut.* **2013**, *82*, 183–188. [[CrossRef](#)]
4. McNutt, L.; Johnson, L.; Kahn, P.; Castillo-Rogez, J.; Frick, A. Near-Earth Asteroid (NEA) Scout. In Proceedings of the AIAA Space Conference and Exposition, San Diego, CA, USA, 4–7 August 2014. [[CrossRef](#)]
5. Spencer, D.A.; Betts, B.; Bellardo, J.M.; Diaz, A.; Plante, B.; Mansell, J.R. The LightSail 2 solar sailing technology demonstration. *Adv. Space Res.* **2021**, *67*, 2878–2889. [[CrossRef](#)]
6. Wilkie, W.K. Overview of the NASA Advanced Composite Solar Sail System (ACS3) Technology Demonstration Project. In Proceedings of the AIAA Scitech 2021 Forum, Virtual Event, 11–21 January 2021; p. 1260.
7. Pezent, J.B.; Sood, R.; Heaton, A.; Miller, K.; Johnson, L. Preliminary trajectory design for NASA's Solar Cruiser: A technology demonstration mission. *Acta Astronaut.* **2021**, *183*, 134–140. [[CrossRef](#)]

8. Oliveira, G.M.C.; Bertachini de A Prado, A.F.; Sanchez, D.M.; Gomes, V.M. Orbital transfers in an asteroid system considering the solar radiation pressure. *Astrophys. Space Sci.* **2017**, *362*, 1–13. [[CrossRef](#)]
9. Prado, A. Minimum Fuel Trajectories for the Lunar Polar Orbiter. *Controle e Automação* **2001**, *12*, 163–170.
10. Arefin, M.A.; Gain, B.; Karim, R.; Hossain, S. A comparative exploration on different numerical methods for solving ordinary differential equations. *J. Mech. Cont. Math. Sci* **2020**, *15*, 1–11.
11. Masood, S.; Naeem, M.; Ullah, R.; Mustafa, S.; Bariq, A. Analysis of the fractional-order delay differential equations by the numerical method. *Complexity* **2022**, *2022*, 1–14. [[CrossRef](#)]
12. Arefin, M.A.; Nishu, M.A.; Dhali, M.N.; Uddin, M.H. Analysis of Reliable Solutions to the Boundary Value Problems by Using Shooting Method. *Math. Probl. Eng.* **2022**, *2022*, 2895023. [[CrossRef](#)]
13. de Almeida, A.K.; Piñeros, J.O.M.; Prado, A.F.B.d.A. On the use of a continuous thrust to find bounded planar trajectories at given altitudes in Low Earth Orbits. *Sci. Rep.* **2020**, *10*, 1–14. [[CrossRef](#)] [[PubMed](#)]
14. Biggs, M. *The Optimisation of Spacecraft Orbital Manoeuvres. Part I: Linearly Varying Thrust Angles*; The Hatfield Polytechnic Numerical Optimisation Centre: Hatfield, UK, 1978.
15. Biggs, M. *The Optimisation of Spacecraft Orbital Manoeuvres. Part II: Using Pontryagin's Maximum Principle*; The Hatfield Polytechnic Numerical Optimisation Centre: Hatfield, UK, 1979.
16. Bryson, A.E.; Ho, Y.C. *Applied Optimal Control: Optimization, Estimation, and Control*; Routledge: Oxfordshire, UK, 2018.
17. Bazaraa, M.S.; Sherali, H.D.; Shetty, C.M. *Nonlinear Programming: Theory and Algorithms*; John Wiley & Sons: New York, NY, USA, 2013.
18. Luenberger, D.G.; Ye, Y. *Linear and Nonlinear Programming*; Springer: New York, NY, USA, 1984; Volume 2.
19. Vulpetti, G.; Johnson, L.; Matloff, G.L. *Solar Sails*; Copernicus Books: New York, NY, USA, 2015; 277p.
20. McInnes, C.R. *Solar Sailing*; Springer Praxis Books: London, UK, 2004; 296p.
21. Wilkie, K. The NASA Advanced Composite Solar Sail System (ACS3) Flight Demonstration: A Technology Pathfinder for Practical Smallsat Solar Sailing. In Proceedings of the 35th Small Satellite Conference, Logan, Utah, 7–12 August 2021.
22. Meireles, L.; Prado, A.; de Melo, C.; Pereira, M. A Study on Different Attitude Strategies and Mission Parameters Based on LightSail-2. *Revista Mexicana de Astronomía y Astrofísica* **2022**, *58*, 23–35. [[CrossRef](#)]
23. The Planetary Society. LightSail 2 Mission Control. 2022. Available online: <https://www.planetary.org/explore/projects/lightsail-solar-sailing/lightsail-mission-control.html> (accessed on 2 February 2023).

Disclaimer/Publisher's Note: The statements, opinions and data contained in all publications are solely those of the individual author(s) and contributor(s) and not of MDPI and/or the editor(s). MDPI and/or the editor(s) disclaim responsibility for any injury to people or property resulting from any ideas, methods, instructions or products referred to in the content.